Liquefaction resistance of Christchurch sandy soil deposits obtained from cyclic direct simple shear tests and CPT-based methods

C. Cappellaro, M. Cubrinovski, G. Chiaro & M.E. Stringer
University of Canterbury, Christchurch, New Zealand

J.D. Bray & M.F. Riemer
University of California, Berkeley, USA

ABSTRACT: Results from cyclic undrained direct simple shear tests on reconstituted specimens of two sands from Christchurch are compared against the liquefaction resistance inferred from CPT-based empirical liquefaction triggering methods. Limitations in existing empirical triggering relationships to capture important effects related to processes which originated test soils are highlighted and discussed.

1 INTRODUCTION

The liquefaction resistance and undrained cyclic response of sands and silty sands under seismic excitation is affected by factors such as soil density, fines content, fabric, and structural features (e.g. layering and segregation) which are related to the formation process and stress history of a soil deposit. Difficulties in retrieving good-quality undisturbed samples of cohesionless soils from the field and the impossibility to replicate in the laboratory the processes leading to the formation of natural soil deposits have represented major obstacles to transfer the results of laboratory investigations on earthquake-triggered soil liquefaction to engineering analyses. This has favoured the development of empirical liquefaction assessment tools based on in-situ investigation methods whose rapidity and simplicity are contrasted by their limited capacity to capture the effects of above mentioned factors.

In-situ investigation techniques and laboratory testing are nevertheless complementary to each other, and their combined use can help to better understand the key factors governing the seismic response of soil deposits. This, in turn, would provide the inputs required to improve the accuracy of predictions achieved by current engineering tools for analysis of earthquake-triggered liquefaction.

During the Canterbury Earthquake Sequence of 2010 and 2011, severe and damaging manifestations of liquefaction associated to natural sands and silty sand deposits of fluvial origin were documented across the Eastern suburbs of Christchurch. In this paper, the results from a series of cyclic undrained direct simple shear (DSS) tests performed on reconstituted specimens of sand from Christchurch are compared against the liquefaction resistance inferred from empirical relationships based on Cone Penetration Testing (CPT). The present work is part of a wider stream of research projects undertaken at the University of Canterbury during the past decade to systematically investigate the liquefaction behaviour of typical soils found in Christchurch, New Zealand, by means of comprehensive field investigations, laboratory tests and advanced numerical analyses.

The DSS device is employed to imitate the mode of deformation undergone by a soil element in the field under earthquake excitation. Soil specimens with different densities are reconstituted in the laboratory using the water sedimentation technique to yield fabric and structure with segregation resembling those encountered in natural fluvial environments. The paper first describes the geologic setting of Christchurch and soil profiles at the sites of interest. Subsequently, test materials and laboratory test procedures are summarized, and DSS test results are presented in terms of liquefaction resistance curves differentiated on the basis of relative density. Liquefaction resistance curves measured in laboratory tests are compared against equivalent curves inferred from CPT-based empirical relationships to scrutinise the limitations of current liquefaction assessment procedures.

2 SITES DESCRIPTION AND SUBSURFACE CHARACTERIZATION

2.1 *Geology of Christchurch*

Key details on Christchurch geologic setting are herein summarized based on the monography by Brown & Weeber (1992). The city of Christchurch is located on the Canterbury plains, which originate

from the progressive accumulation of Quaternary alluvial sediments transported by rivers flowing from the Southern Alps eastwardly into the Pacific Ocean. In the proximity of the coast, as a result of alternating sea transgression and regression events which took place over geologic time, these alluvial deposits interfinger with marine soil formations. In the last sea transgression event, the coastline reached its inland limit west of the Central Business District (CBD) of Christchurch about 6500 years B.P. before gradually retroceding to its current position, as sea levels decreased (Figure 1).

The shallowest formations found in the Christchurch area are:

- Riccarton Gravel: glacial deposit a few meters up to 20 m thick located 10 to 40 m below the ground surface;
- Christchurch Formation: beach, estuarine, lagoonal dune and coastal swamp deposits associated with the last marine transgression event.
- Springston Formation: postglacial fluvial channel and overbank sediments accumulated at the inland margin of the Christchurch Formation.

Essentially, as one moves from the city centre towards the coast, the Springston Formation becomes progressively thinner while the top of the underlying Christchurch Formation approaches the ground surface. Superimposed on this trend, however, one encounters significant variability at a site scale in soil deposits and geomorphologic conditions. Manifestations of liquefaction observed during the 2010-2011 Canterbury Earthquake Sequence were associated with deposits of sands, silty sands and sandy silts comprised within the Christchurch and Springston formations (Cubrinovski and Green 2010, Cubrinovski et al. 2011).

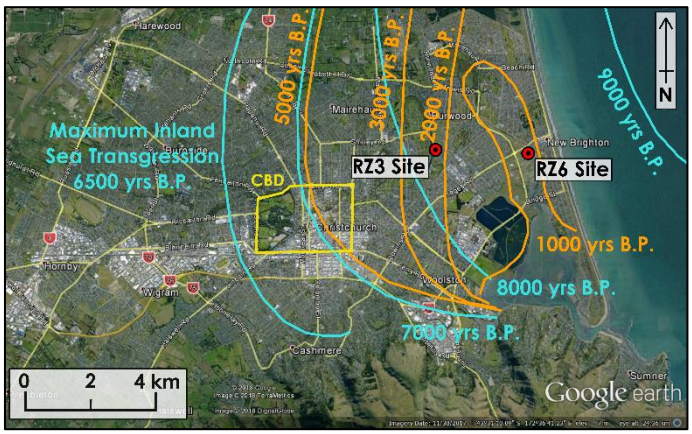

Figure 1. Sea level changes in the Christchurch area (contours from Brown & Weeber 1992 on Google Earth Map with Data from DigitalGlobe 2018 and TerraMetrics 2018).

2.2 *Sites description*

The two sites considered in this paper are located in the Red Zone of Christchurch, along the riverbanks of the Avon River, and will be identified as RZ3 and RZ6 (Figure 1). Major and repeated manifestations of liquefaction, which caused severe damage to buildings and infrastructure, were documented across the Red Zone during the Canterbury Earthquake Sequence.

As part of a broader research program involving several institutions including the University of Canterbury and the University of California, Berkeley (e.g. Beyzaei et al. 2018), the RZ3 and RZ6 sites have been extensively characterized by means of borehole logging and in-situ tests (CPT, SDMT, shear wave velocity profiling), and undisturbed samples have been retrieved to determine the liquefaction resistance of sensitive layers by means of cyclic triaxial tests. CPT traces of cone tip resistance, q_c, and Normalized Soil Type Behaviour Index, I_c, for the two sites are shown in Figure 2, together with computed values of normalized equivalent clean sand cone tip resistance, $q_{c1N,cs}$ (Boulanger & Idriss, 2016). These CPT data were retrieved from the New Zealand Geotechnical Database (NZGD).

The stratigraphy of both sites can be represented as a silty sand layer, about 2 m thick, capping thicker sand deposits with I_c values generally less than 2.0. The ground water table at both sites is located within the cap layer. Observed variations among CPT logs, which at each site are spaced 5-10 m from each other, are related to local variability in soil stratigraphy.

Values of q_c measured at the RZ3 site are pretty consistent up to 6-7 m depth before showing a higher degree of variability, and computed $q_{c1N,cs}$ values for the sand layer between 3-6 m depth range between 110-140. At the RZ6 site, computed $q_{c1N,cs}$ values between 5-10 m depth fall in the range 150-200. In the upper part of the sand layer (2-5 m depth), two CPT profiles show $q_{c1N,cs}$ values of 100-120, while the other two attain higher values of normalized equivalent clean sand cone tip resistance.

3 EXPERIMENTAL DETERMINATION OF LIQUEFACTION RESISTANCE

3.1 *Test soil*

Test materials consist of (Figure 2):

- Downhole sample from the RZ3 site retrieved at 5.7 m depth (sand layer);
- Bulk sample from the RZ6 site retrieved at 1.7 m depth (silty sand cap layer). In this case, the fraction passing the 75 μm sieve was removed by dry sieving, and the resulting clean sand used in subsequent tests.

Particle size distribution curves of test soils are shown in Figure 3, while their index properties are listed in Table 1. Both test sands present sub-angular to sub-rounded particles, although more detailed investigations onto particle shape and angularity of test soils are currently in progress.

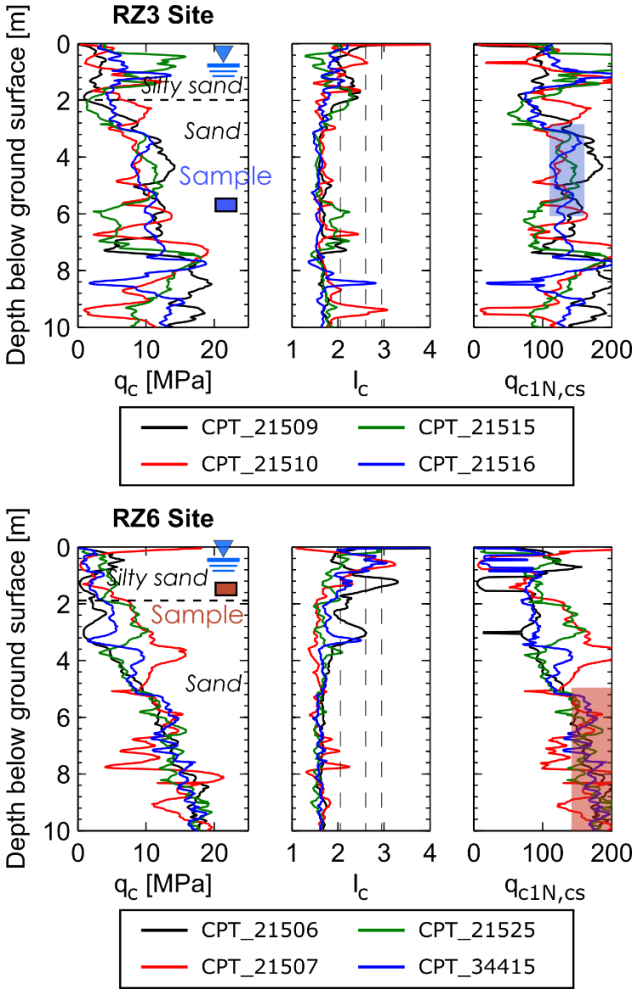

Figure 2. CPT profiles of q_c, I_c and $q_{c1N,cs}$ for the two sites of interest in Eastern Christchurch (data from NZGD), and location of soil samples used in DSS testing series.

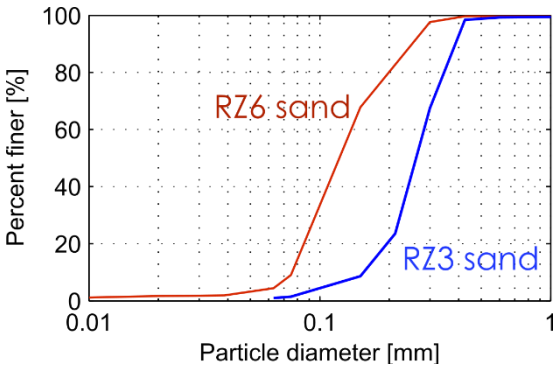

Figure 3. Particle size distribution curves of test sands from wet sieve analyses.

Table 1. Index properties of RZ3 and RZ6 sand.

Site	G_s	e_{min}	e_{max}	D_{50}
				mm
RZ3	2.66	0.59	0.99	0.27
RZ6	2.66	0.69	1.19	0.13

Notice that the residual fines content in RZ6 sand after dry sieving is 9%. Lab test results (unpublished data) show that fines content for this specific soil plays a secondary role on its liquefaction resistance and undrained stress-strain behaviour. For this reason, RZ6 sand will treated herein as a clean sand, although its fines content is slightly above 5%.

Other samples retrieved at the RZ6 site between 4 and 6 m depth (University of California, Berkeley & University of Canterbury 2016) presented the following characteristics:

- Fines content less than 5%;
- D_{10} = 0.15-0.17 mm, D_{50} = 0.23-0.24 mm and D_{60} = 0.25-0.26 mm;
- e_{min} = 0.63-0.64 and e_{max} = 1.04-1.06;

Similarities in these properties with those shown above for the RZ3 sample, comparisons between layer depth and location of the sites, and radiocarbon samples from Christchurch (Brown and Weeber 1992) suggest that the sand from the RZ3 site tested in DSS and sands below 4 m depth at the RZ6 site were deposited in similar depositional environments – in particular, they should both belong to the Christchurch Formation. This aspect is of particular importance considered the very different undrained cyclic response observed in DSS tests on the two clean sands (i.e. natural sand from RZ3 site and sieved sand from RZ6 site).

3.2 *Cyclic DSS testing for liquefaction evaluation: testing equipment, procedures and results*

Cyclic DSS testing is used to study the undrained cyclic soil response by subjecting the test specimen to a mode of deformation similar to that of a soil element in level-ground, free field conditions under earthquake excitation (Figure 4). DSS tests performed on RZ3 and RZ6 sands are described in detail in Cappellaro et al. (2018), and only a brief description of testing features relevant for the present discussion will be reported herein.

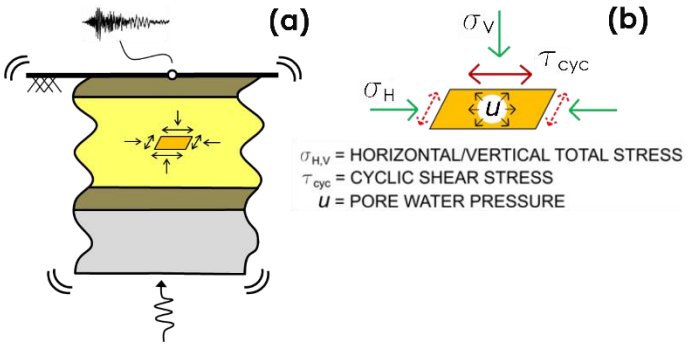

Figure 4. (a) Model of propagation of SH seismic waves through level ground, free-field soil deposit and (b) stresses imposed on specimen in cyclic DSS test.

Test soils were used to prepare reconstituted specimens using the water sedimentation technique. In comparison to other specimen preparation methods, this technique is deemed to better reproduce soil fabric (i.e. orientation of particle grains) and structural features such as segregation resulting from water depositional environments as those found in Christchurch. The technique involves pouring dry soil into a mould filled with water, yielding a specimen in a loose state. Denser initial states are achieved by placing additional weights on top of the specimen and by applying gentle vibrations to the table on which the mould is resting. The initial relative densities achieved with this methodology range from 50 to 80% for RZ3 sand, and from 65 to 80% for RZ6 sand. It is noteworthy that the lowest initial relative density attained by RZ6 sand with this procedure is significantly higher than that attained by RZ3 sand, and that the subsequent densification process by vibration yields a relatively limited increase in relative density for RZ6 sand.

The DSS device used in this tests is provided with a confining pressure chamber which allows control of the horizontal total stress imposed onto the specimen and to use back pressures for specimen saturation, similarly to a triaxial device. After saturation, specimens are consolidated anisotropically, at σ'_{v0} = 100 kPa and σ'_{h0} = 50 kPa. Specimens are sheared under a sinusoidal shear load waveform of pre-determined amplitude at a frequency of 0.05 Hz. Shearing takes place in undrained conditions (drainage valves are closed) at constant cell pressure, $\sigma_h = \sigma_{cell}$, while the height of the specimen is also maintained constant. Boulanger (1990) has shown the equivalence of these conditions to those of a test under constant total vertical stress, which is the stress condition effectively encountered in the field.

Test data on liquefaction resistance for the two sands are presented in Figure 5. The applied cyclic stress ratio, CSR, is given by:

$$\mathrm{CSR} = \frac{\tau_{cyc}}{\sigma'_{v0}} \quad (1)$$

where τ_{cyc} = applied cyclic shear stress and σ'_{v0} = initial vertical effective stress. Liquefaction is defined as the attainment of 7.5% DA (double-amplitude, i.e. peak-to-peak) shear strain, a condition which in clean sands corresponds closely to the condition r_u = 1.0, with:

$$r_u = \frac{\Delta u}{\sigma'_{v0}} \quad (2)$$

where Δu = excess pore water pressure generated during the test.

Test results for RZ3 sand are fitted by two distinct liquefaction resistance curves for different relative densities (which are related to vibration time during specimen preparation). On the other hand, given the limited changes in relative density and liquefaction resistance observed in RZ6 sieved sand following the vibration process, all test data for this sand are fitted by a single liquefaction resistance curve, independently from vibration time and relative density.

4 CPT-BASED LIQUEFACTION RESISTANCE CURVES

The CPT-based assessment procedure, commonly referred to as the "simplified method", represents the standard tool for the assessment of seismically-induced soil liquefaction in engineering practice. It was developed in order to provide engineering practitioners with a relatively inexpensive tool to use in ordinary applications, while more difficult and expensive tasks involving undisturbed field sampling and laboratory testing remain confined to research investigations or to major projects. Different implementations of the simplified method exist which differ essentially for the equations used in calculations, while they share many fundamental assumptions. The analysis presented in this paper follows the CPT-based liquefaction assessment procedure as implemented by Boulanger & Idriss (2016).

CPT-based liquefaction assessment assumes that factors (particle size distribution and mineralogy, relative density, soil fabric and structure, ageing and

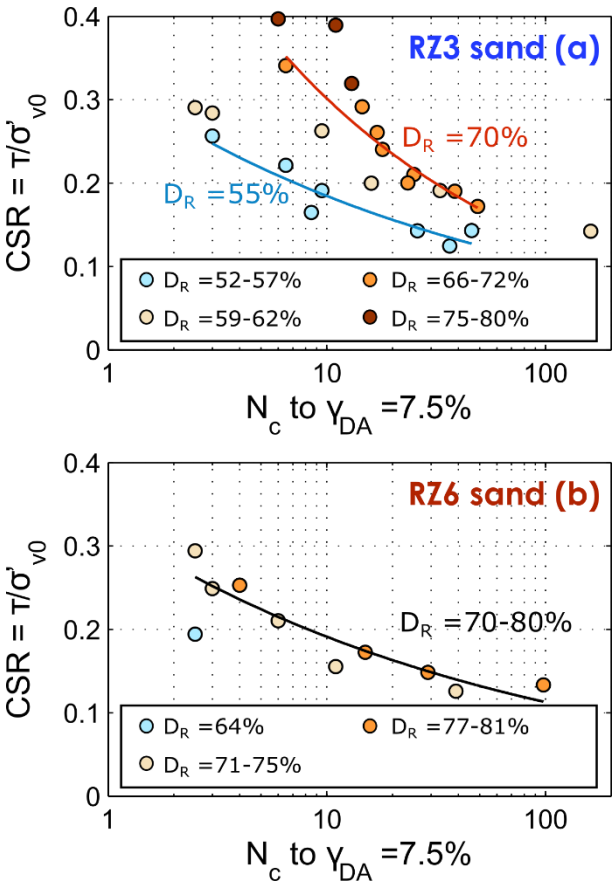

Figure 5. DSS test results: liquefaction resistance (as number of cycles to 7.5% DA shear strain) of specimen reconstituted by water sedimentation of (a) RZ3 sand and (b) RZ6 sand.

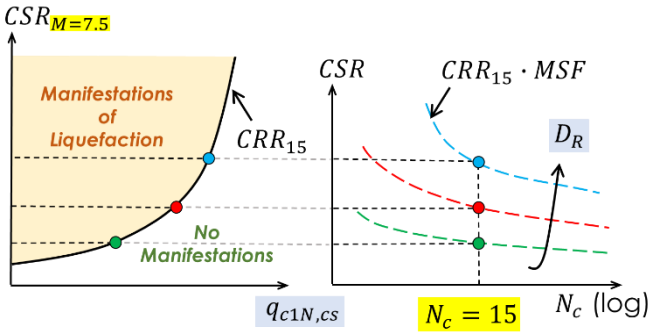

Figure 6. Relationship between CPT-based liquefaction assessment and liquefaction resistance curves from laboratory tests.

seismic stress history, among others) which would increase the liquefaction resistance of a soil deposit would also result in an increased cone tip resistance, q_c, measured in that deposit (Tokimatsu 1988). For the purposes of liquefaction assessment, q_c is translated into a normalized equivalent clean sand cone tip resistance, $q_{c1N,cs}$, following theoretical and empirical studies on the effects of relative density, confining stress and fines content on soil behaviour and cone tip resistance.

The CPT-based procedure is usually presented in the form of a chart (Figure 6) based on no-liquefaction and liquefaction observations recorded at case history sites during past earthquakes. In developing this chart, each study site has been associated to the $q_{c1N,cs}$ value for the weakest soil layer in the underlying soil deposits (the *critical layer*), and the boundary curve separating liquefaction and no-liquefaction observations defines the liquefaction resistance for a M_w7.5 earthquake. The demand imposed by the earthquake is considered to be equivalent to a series of N_c shear stress cycles of uniform amplitude CSR, with N_c = 15 for M_w = 7.5. For a number of cycles N_c other than 15 (i.e. for moment magnitudes different from 7.5), CRR_{15} is multiplied by a Magnitude Scaling Factor, MSF, which is a function of relative density D_R – a dependency introduced to capture trends observed in element-level (triaxial, direct simple shear, torsional) cyclic laboratory tests. In calculations, D_R is actually replaced by $q_{c1N,cs}$ based on the relationship between $q_{c1N,cs}$ and D_R proposed by Salgado et al. (1997).

From this discussion, it is apparent that a series of liquefaction resistance curves is implicitly embedded within the CPT-based assessment procedure (Figure 6). This feature may not be readily apparent to the user of the method, as the explicit derivation of the curves is not required when performing calculations for liquefaction triggering assessment.

5 COMPARISONS AND DISCUSSION

Figure 7 shows CPT-based liquefaction resistance curves for $q_{c1N,cs}$ values of 100, 120, 140 and 160 (black dashed lines), for which equivalent relative densities have been computed using the $q_{c1N,cs}$-D_R relationship of Salgado et al. (1997). These curves indicate the number of stress cycles necessary to observe manifestations of liquefaction in the field. Liquefaction resistances for CPT data from the RZ3 site at 3-6 m depth (blue shading) and from the RZ6 site below 5 m depth (red shading) are also marked onto this figure. Experimental DSS liquefaction resistance curves for RZ3 sand (blue lines) and RZ6 sieved sand (red line), first presented in Figure 6, are included for comparison. These latter curves indicate the number of stress cycles necessary to attain a certain threshold value of shear strains in the DSS tests.

In general, laboratory tests provide information on soil behaviour in terms of stress-strain response and generation of excess pore water pressure, which provide quantitative definitions of liquefaction resistance. This can be contrasted with the empirical triggering curves, which are based on a binary description of performance (presence or no-presence of sand ejecta) of a whole soil deposit, not of a single layer (even in the case of the critical layer). Surface manifestations of sand boils at the surface involve redistribution of excess pore water pressures across layers, and the response of a specific layer depends on liquefaction strength and permeability of neighbouring layers (Pender et al. 2016, Cubrinovski et al. 2017, Green et al. 2018). However, in the current formulation of the simplified method, empirical triggering curves are applied separately to each layer in a deposit, and these estimates of liquefaction resistance used in subsequent calculations of post-liquefaction deformations neglecting layer-to-layer interaction (Cubrinovski et al. 2017).

The boundary curve from the CPT-based liquefaction assessment procedure is an envelope of liquefaction case histories, and should therefore represent a lower bound to the liquefaction resistance of soils with any fabric. One would expect this condition to be met especially in the case of clean sands, as they represent the reference soil in triggering procedures and are not affected by the huge uncertainties which relationships between CPT parameters and fines content usually involve. Nevertheless, the DSS liquefaction resistance curve for RZ6 sieved sand, D_R = 70-80% (red line), in Figure 7 plots well below the empirical curves (black dashed lines) for similar values of equivalent relative density, and is also significantly lower than the resistance of RZ3 sand prepared at D_R = 70%. RZ3 sand experimental curves are instead in agreement with the expectation that CPT-derived curves should provide a lower-bound estimate to liquefaction resistance. This suggests that factors other

than relative density which are not properly accounted for by empirical triggering procedures actually play an important role in determining the liquefaction resistance of RZ6 sieved sand.

One notices then that CPT-derived liquefaction resistance of natural clean sands at the RZ6 site between 5-10 m depth (red shaded area) is significantly higher than the resistance measured in DSS on RZ6 sieved sand (red line), which was sampled from the silty sand layer in the top 2 m at that site. The CPT-derived liquefaction resistance for natural clean sand deposits at the RZ6 site (red shaded area) is actually consistent with the DSS resistance determined on RZ3 sand specimens (blue lines) sampled at 5.7 m depth. This can be linked back to the initial observation that these sands originate from the same geologic formation and presumably present analogous depositional environment effects on particle gradation, shape and angularity, which in turn affect liquefaction resistance. However, the differences in behaviour related to these factors are not captured by current formulations of the simplified method.

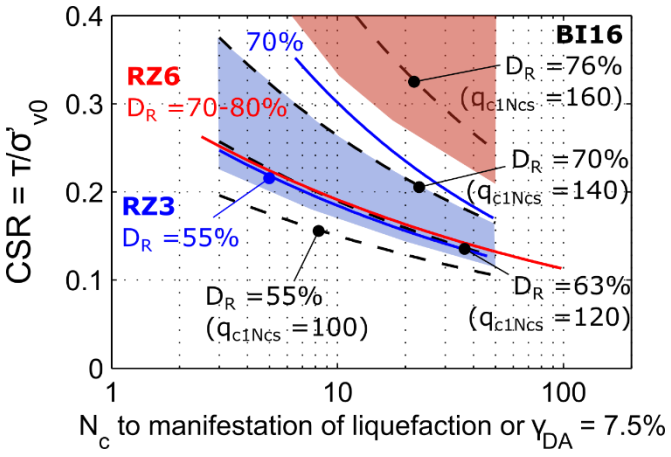

Figure 7. Liquefaction resistance curves from CPT-based assessment procedure (BI16) and DSS tests on two sands from Christchurch. Shaded areas refer to $q_{c1N,cs}$–based curves for sand layers at the RZ3 and RZ6 sites (data in Figure 2).

6 CONCLUSIONS

The liquefaction resistance of two sands sampled at two different sites in Christchurch, New Zealand, was determined using DSS tests on reconstituted specimens and compared against the liquefaction resistance inferred from the CPT-based liquefaction triggering procedure. Significant differences in the liquefaction resistance of the two sands, possibly related to different processes which originated their source deposits, were not captured by the simplified method. Better quantification of depositional environment and soil fabric effects on liquefaction resistance will be pursued within the present research project by means of future tests on high-quality undisturbed samples of the same soils used herein to prepare reconstituted specimens.

ACKNOWLEDGEMENTS

The authors would like to acknowledge the financial support provided by the Earthquake Commission (EQC), the Natural Hazards Research Platform (NHRP), and the College of Engineering, UC Berkeley through the Chair in Earthquake Engineering Excellence. The help and assistance from the lab technicians at the University of Canterbury, Mr Siale Faitotonu, Ms Nicole van de Weerd and Mr Michael Weavers, are gratefully acknowledged. The CPT profiles were retrieved from the New Zealand Geotechnical Database. The first author wishes to thank the support to his studies provided by the UC Doctoral Scholarship and by QuakeCoRE.

REFERENCES

Beyzaei, C.Z., Bray, J.D., Cubrinovski, M., Riemer, M. & Stringer, M. 2018. Laboratory-based characterization of shallow silty soils in southwest Christchurch. *Soil Dyn. Earthq. Eng.* 110: 93-109.

Boulanger, R.W. 1990. *Liquefaction Behavior of Saturated Cohesionless Soils Subjected to Uni-Directional and Bi-Directional Static and Cyclic Simple Shear Stresses*. PhD Thesis, University of California, Berkeley.

Boulanger, R.W. & Idriss, I.M. 2016. CPT-Based Liquefaction Triggering Procedure. *J. Geotech. Geoenv. Eng.* 142(2).

Brown, L. & Weeber, J. 1992. *Geology of the Christchurch urban area*. Institute of Geological and Nuclear Sciences, Lower Hutt, New Zealand.

Cappellaro, C., Cubrinovski, M., Bray, J.D., Chiaro, G., Riemer, M.F. & Stringer M.E. 2018. Comparisons in the Cyclic Direct Simple Shear Response of Two Sands from Christchurch, New Zealand. In Brandenberg & Manzari (eds.) *Proc. GEESD V, Austin, 10-13 June 2018*. ASCE.

Cubrinovski, M., Bradley, B., Wotherspoon, L., Green, R. A., Bray, J. D., Wood, C., … Wells, D. (2011). Geotechnical Aspects of the 22 February 2011 Christchurch Earthquake. *Bull. NZSEE* 44(4): 205-226.

Cubrinovski, M. & Green R.A. (eds.) 2010. Geotechnical Reconnaissance of the 2010 Darfield Earthquake. *Bull. NZSEE* 43(3): 243-320.

Green, R.A., Maurer, B.W. & van Ballegooy, S. 2018. The Influence of the Non-Liquefied Crust on the Severity of Surficial Liquefaction Manifestations: Case History from the 2016 Valentine's Day Earthquake in New Zealand. In Brandenberg & Manzari (eds.) *Proc. GEESD V, Austin, 10-13 June 2018*. ASCE.

Pender, M.J., Orense, R.P, Wotherspoon, L.M. & Storie, L.B. 2016. Effect of permeability on the cyclic generation and dissipation of pore pressures in saturated gravel layers. *Géotechnique* 66(4): 313-322.

Salgado, R., Boulanger, R. W., & Mitchell, J. K. 1997. Lateral stress effects on CPT liquefaction resistance correlations, *J. Geotech. Geoenv. Eng.*, 123(8): 726–35.

Tokimatsu, K. 1988. Penetration tests for dynamic problems. In De Ruiter (ed.), *Penetration Testing 1988, ISOPT-1*. Rotterdam: Balkema.

University of California, Berkeley & University of Canterbury in collaboration with Tonkin + Taylor, Ltd. 2016. *Liquefaction Triggering & Consequence of Low-Plasticity Silty Soil Sites in Christchurch during the Canterbury Earthquake Sequence*. Data reports prepared for the NZ Ministry of Business, Innovation and Employment.